

**ECONOMIC GEOLOGY
RESEARCH UNIT**

University of the Witwatersrand
Johannesburg



**THE CANDELARIA COPPER-GOLD DEPOSIT,
CHILE**

**P.J. RYAN, A.J. LAWRENCE, R.A. JENKINS,
J.P. MATTHEWS, J.C. ZAMORA, E. MARINO W,
and I.U. DIAZ**



INFORMATION CIRCULAR No. 301

UNIVERSITY OF THE WITWATERSRAND
JOHANNESBURG

**THE CANDELARIA COPPER-GOLD DEPOSIT,
CHILE**

by

**P.J. RYAN¹, A.J. LAWRENCE¹, R.A. JENKINS², J.P. MATTHEWS³
J.C. ZAMORA⁴, E. MARINO W⁴ and I.U. DIAZ⁴**

(¹ *Phelps Dodge Corporation, Phoenix, Arizona, U.S.A.*

² *Phelps Dodge Mining Co., Santiago, Chile*

³ *Phelps Dodge Co., Tucson, Arizona, U.S.A.*

⁴ *CCM Ojos del Salado, Santiago, Chile*

**ECONOMIC GEOLOGY RESEARCH UNIT
INFORMATION CIRCULAR No. 301**

August, 1996

ACKNOWLEDGEMENT

INFORMATION CIRCULAR No. 301

The information contained herein has previously appeared in:
F.W. Pierce and J.G. Bolm (Editors), **Porphyry Copper Deposits
of the American Cordillera**, published by the Arizona Geological
Society, Digest 20 (1995), p.625-645.

_____oOo_____

THE CANDELARIA COPPER-GOLD DEPOSIT, CHILE

ABSTRACT

The Candelaria Deposit is located near the town of Tierra Amarilla in the Atacama Desert, Region III, Chile. It was discovered in 1987 by Phelps Dodge Mining Company. Minable reserves are estimated at 366 million tonnes averaging 1.08% copper and 0.26 g/t gold. Mineralization consists of magnetite, chalcopyrite, gold-rich electrum, and pyrite and is hosted in skarned and biotitized volcanics and sediments of Cretaceous age. The mineralization occurs as veins, breccia fillings, and fine- to coarse-grained disseminations. The deposit reaches a thickness of over 350 m near its center and thins outwards into manto-like bodies. A series of north-northwest-trending faults cut the mineralization.

The formation of the deposit involved a complex series of structural, metamorphic, and metasomatic events. There was an early period of potassium metasomatism accompanied by chalcopyrite-magnetite mineralization. This was followed by shearing and skarn formation caused by contact metamorphism and iron metasomatism. Next there was a second phase of skarn formation that caused the replacement of many of the earlier-formed skarn minerals by sodium-rich scapolite and hedenbergitic clinopyroxene. This was accompanied by remobilization of magnetite and chalcopyrite and deposition of pyrrhotite. Retrograde metamorphism followed with partial replacement of earlier skarn minerals by amphibole, chlorite, epidote, clinozoisite, and minor sericite. Last appears to have been the overprinting and partial replacement of all previously formed assemblages by potassium feldspar.

No igneous source of the mineralization has been found, and no clearly defined zonation of either alteration or mineralization has been recognized. The complex metamorphic and metasomatic history of the deposit has apparently redistributed the mineralization and destroyed much of the information needed to determine its origin. The large size, simple mineralogy, and association of early mineralization with potassic alteration suggest that the deposit may have originally been a deep-seated porphyry copper deposit.

_____oOo_____

THE CANDELARIA COPPER-GOLD DEPOSIT, CHILE

CONTENTS

	Page
INTRODUCTION	1
History of the Discovery	1
REGIONAL GEOLOGIC SETTING	5
LOCAL GEOLOGY	6
Volcanic and Sedimentary Rocks	6
Intrusive Rocks	6
Contact Metamorphism and Metasomatism	7
Structural Geology	8
Stratigraphy	8
<i>Lower Andesites</i>	8
<i>Tuffs or Volcaniclastic Sediments</i>	9
<i>Upper Andesites</i>	10
<i>Metasedimentary Rocks</i>	10
<i>Intrusive Rocks</i>	11
<i>Quaternary Sediments</i>	11
Structural Geology	11
MINERALIZATION AND ALTERATION	13
Ore Mineralogy	13
<i>Magnetite</i>	13
<i>Pyrite</i>	14
<i>Chalcopyrite</i>	15
<i>Gold</i>	15
<i>Pyrrhotite</i>	15
<i>Marcasite</i>	16
<i>Sphalerite</i>	16
<i>Galena</i>	16
<i>Hematite</i>	16
<i>Ilmenite</i>	16
<i>Cubanite</i>	17
<i>Arsenopyrite</i>	17
<i>Molybdenite</i>	17
<i>Anhydrite and Gypsum</i>	17
<i>Paragenesis of Opaque Minerals</i>	17
<i>Orebodies</i>	17
<i>Alteration</i>	21
<i>Skarns</i>	22
<i>Stages of Skarn Development</i>	24
<i>Deposit Origin</i>	24

THE CANDELARIA COPPER-GOLD DEPOSIT, CHILE

CONTENTS (continued)

	Page
CONCLUSIONS	24
ACKNOWLEDGEMENTS	25

____ oOo ____

Published by the Economic Geology Research Unit
Department of Geology
University of the Witwatersrand
1 Jan Smuts Avenue
Johannesburg 2001
South Africa

ISBN 1 86838 231 1

THE CANDELARIA COPPER-GOLD DEPOSIT, CHILE

INTRODUCTION

The Candelaria Copper-Gold Deposit is located about 20 km south of the town of Copiapó in the Atacama Province, Region III, Chile (Fig. 1). It is situated 800 km north of Santiago and 75 km from the Pacific Ocean. The town of Tierra Amarilla and the Punta del Cobre Mining District lie 4 km to the northeast. The top of the deposit is at an elevation of around 500 m above sea level. Mineralization is beneath and along the west slope of Quebrada Los Bronces to the west of Sierra El Bronce. The Copiapó River valley lies about 2 km to the east.

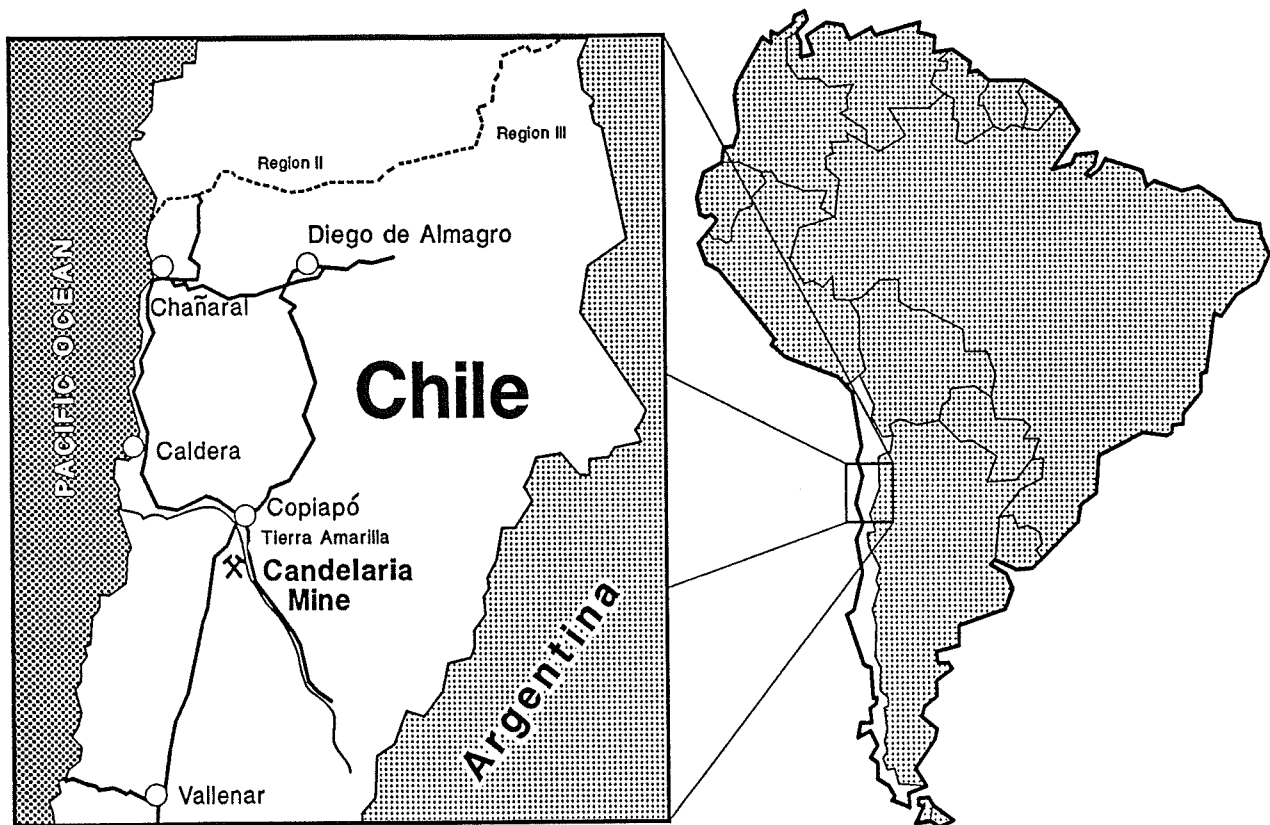


Figure 1: Map showing location of the Candelaria Copper-Gold Deposit in Chile.

Minable reserves are estimated at 366 m/t at an average grade of 1.08% copper and 0.26 g/t gold using a 0.4% copper cut-off grade. The deposit will be brought into production at an initial milling rate of 28,000 t per day.

History of the Discovery

The only recorded mining activity in the area of the Candelaria Deposit was a small copper prospect first staked in the 1930's and subsequently abandoned. In 1969 the deposit was restaked as the Violeta Prospect and then again abandoned. The property was restaked

in 1981 as the Lar Claim and mined on a small scale for copper-oxide ore. Phelps Dodge's involvement in the Candelaria project area dates back to 1983 when Compania Minera Ojos del Salado, a wholly owned subsidiary, first leased the Lar property and mined about 1,800 tonnes of oxide-copper-gold ore from the small outcropping manto deposit. A drilling program recommended by the Ojos del Salado geological department to explore for sulfide ores was not carried out, and the property was dropped in early 1984 because of poor metallurgical recovery of gold from the oxide ores. In 1985, as a result of diminishing ore reserves, it was clear to Phelps Dodge management that additional ore would be required to keep the Ojos del Salado concentrator in operation. Phelps Dodge exploration geologists immediately began work in the area and recommended further study of the Lar property. The Lar property was re-optioned in late 1985, and a percussion drilling program was carried out to explore for sulfide ore downdip from the outcropping copper oxides of the Lar Manto. This program outlined a small manto-like sulfide copper-gold ore body at the Lar Mine and another at the Bounce Mine 1 km to the south. A percussion hole was drilled a few hundred meters to the southwest of the Lar Mine in an effort to expand the area of known mineralization. This hole encountered a few meters of chalcopyrite mineralization at a depth of 70 m but had to be abandoned due to a heavy inflow of water.

While the Lar and Bounce Deposits were being mined, exploration was conducted elsewhere on the property. The initial induced polarization (IP) survey completed in late 1986 over an area including the Lar and Bounce Mines was designed to determine the response of the known mineralization and look for extensions or additional ore bodies. An anomalous zone that trends roughly north-northeastward from the Bounce Mine to the Lar Mine was delineated (Fig. 2). One line, 700 N, was located to test the area where the earlier percussion drilling had intersected low grade sulfide mineralization at a depth of 70m. A well-defined IP anomaly at depth indicated that significant mineralization could be present below the area previously drilled. In February of 1987 the anomaly was tested with a diamond drill hole which intersected more than 50 m of mineralization averaging almost 2% copper with significant gold. Following the discovery of substantial ore-grade mineralization in this first hole, additional IP surveys were run using both 50 and 100 m dipole spacings and a line separation of 100 m. The follow-up surveys showed an interesting anomaly located about 1 km to the southwest of the discovery hole. Testing of this anomaly by diamond drilling led to the discovery of the South Candelaria Deposit. Subsequent fill-in drilling showed that this area was connected by low grade mineralization to the initial area as had been suggested by IP.

Ground magnetic surveys with readings taken every 25 m were carried out on the same grid. The magnetics showed that the deposit was located on a strong magnetic gradient with rocks of lower magnetic susceptibility to the southeast and higher magnetic susceptibility to the northwest (Fig. 3). The deposit was located within a broad contact metamorphic-metasomatic halo on the east flank of the Andean Batholith. This contact halo contains abundant disseminated pyrite which produces extensive IP anomalies.

In 1988 a regional aeromagnetic survey was flown which covered the entire district. This correlated well with the ground magnetic data at Candelaria, and several other deposits in the district were also shown to be associated with high susceptibility rocks. Follow-up on one of the magnetic highs led to the discovery of the previously unknown Alcaparrosa Deposit which is presently under development by Ojos del Salado.

Candelaria Deposit

Induced Polarization Response (IP)

Survey Date: Nov. 1987

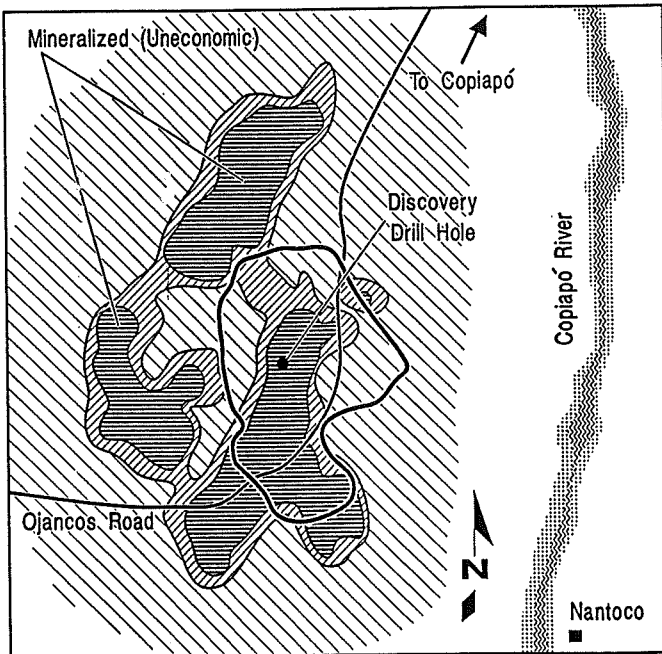
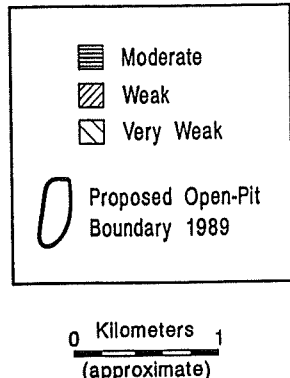


Figure 2: Plan of the induced polarization response (IP) within the Candelaria area. Both copper-rich and pyrite-rich mineralization exhibit similar IP responses. The spatial relationship of mineralization to the discovery hole and the open pit are also shown.

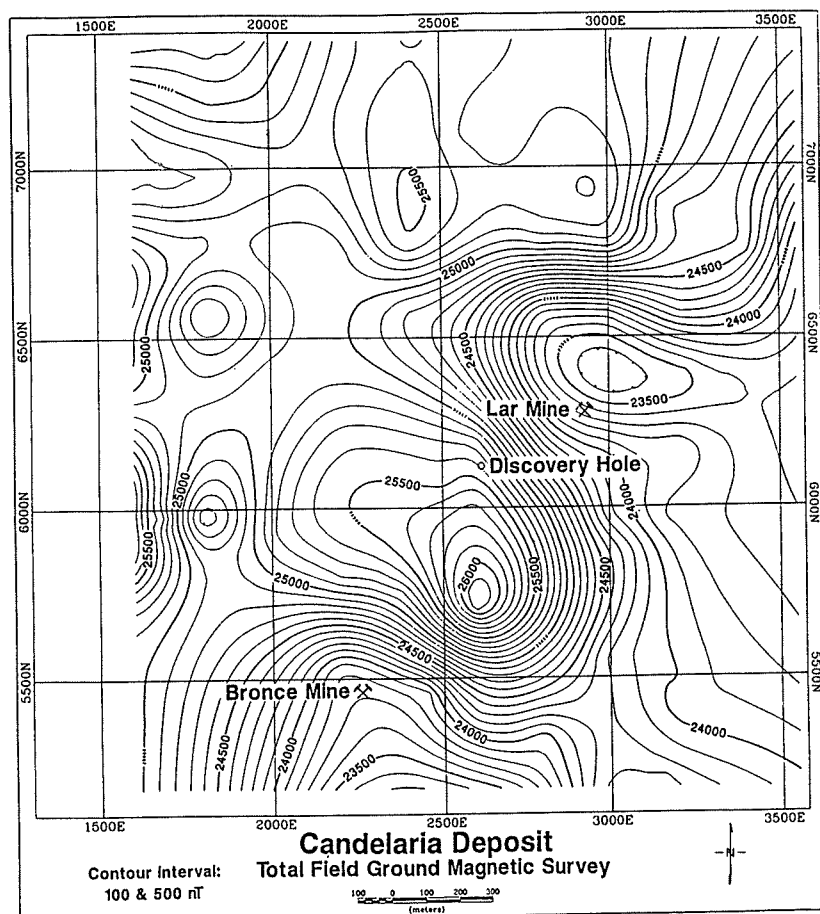


Figure 3: Contour map of total field ground magnetic data in a portion of Candelaria. The Candelaria Deposit is on a magnetic high located along a gradient between higher susceptibility rocks to the northwest and lower susceptibility rocks to the southeast.

The Candelaria Deposit exhibits an IP response similar to that of surrounding more pyritic areas. It was therefore fortunate that the initial geophysical surveys were concentrated in the area of the Lar and Bronce Mines, which led to a target and discovery hole early in the program. That ore-grade mineralization is in stacked mantos was also fortuitous, because detection of shallow mineralization was a pathfinder to deeper and often better grade mineralization at depth.

The project area was covered by 215 line-kilometers of IP and ground magnetic surveys during the initial exploration phase. The area around the deposit was covered by over 16 km² of geologic mapping at a scale of 1:5 000, and the central 3 km² overlying the deposit were mapped at a scale of 1:2 000.

During the exploration and orebody delineation phases of the project (1987 to 1990), 325 holes were drilled on a grid with holes spaced every 50 m in the area of the main deposit and every 100 to 400 m in the peripheral areas. Approximately 36,6 km of percussion drilling and 98,6 km of diamond drilling were completed during the project. Drilling was used to delineate the ore body and select areas for tailings, low grade and barren rock stockpiles, plant sites, and other ancillary facility sites. Because of abundant magnetite in the ore and wall rocks, deviations of all drill holes were measured using a gyroscope probe. All drill core was logged for rock type, alteration, ore type, and rock mechanics properties. More than 70 000 density measurements and over 80 000 analyses for copper, gold, and silver were performed. To prove lateral continuity of mineralization and to obtain representative samples of different ore types for metallurgical testing, 2 090 m of underground workings were driven. These workings were mapped and sampled in detail. Both vertical and horizontal channel samples were taken in the mineralized areas. Each blasted round from the exploration decline was stockpiled separately, and bulk samples were taken for assay and density determinations. Stockpiles were labeled according to ore type and grade. The work done on the exploration decline proved the continuity of ore distribution and grade. It also provided close-spaced near-horizontal data for determining the variability of the orebody. Representative samples of the total orebody and each ore type were prepared separately for pilot plant testing. During 1989 a total of 72 455 t of ore were processed at the nearby Ojos del Salado concentrator. This large-scale test work showed that the metallurgical properties and recoveries of all of the ore types were similar and that recoveries in excess of 90 percent could be expected.

With completion of metallurgical test work and exploration drilling, geologic and orebody models were constructed using data from over 300 drill holes and 2 090 m of underground workings. A total of about 55 cross-sections and longitudinal sections were hand drawn to build the geologic model and a similar number of cross sections and longitudinal sections were drawn to produce the orebody model. In order to provide cross-sections that cut the ore body and associated structures at close to right angles, sections were constructed across the diagonal of the drill grid. This produced a spacing between the sections of about 35 m with drill holes separated by about 70 m along each section. All the sections were digitized, and a computer generated geologic model was constructed using Datamine software. Geology and orebody limits were used to constrain the limits of the individual ore zones.

All assays were weighted using measured specific gravity. If no measured value was available, the average specific gravity for the same lithologic or ore type was used. The same procedure was used for waste rock using the average specific gravity for each lithologic type in non-mineralized areas.

Both hand generated and computer generated ore reserve calculations were done using a 0.4% copper cut-off grade. The two methods produced reserves within 10% of one another in both tonnage and grade, with the computer generated reserves giving more tons at a lower grade. The total contained copper derived from the two calculations was almost the same.

REGIONAL GEOLOGIC SETTING

The regional geology of the Copiapó area consists of a coastal batholith of Jurassic-Cretaceous age that intrudes a basement formed of Upper Paleozoic accretionary prism rocks and Permian intrusives (Brown, 1987; Mpodozis and Allmendinger, 1992; Fig. 4). The

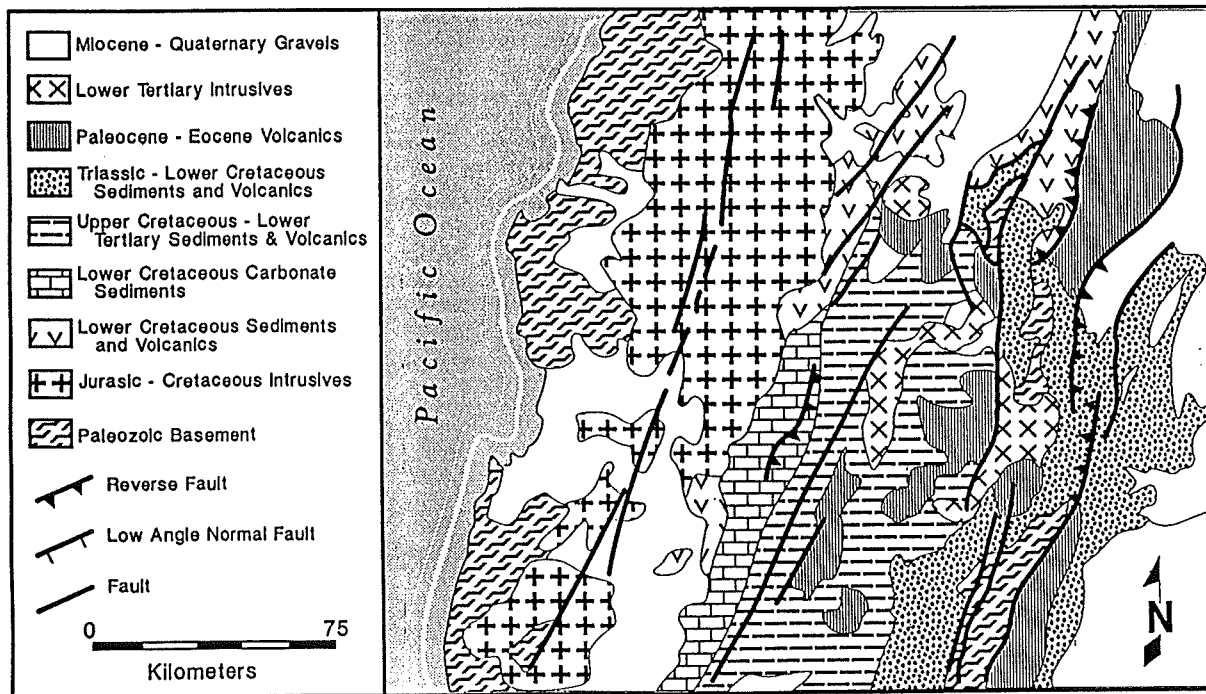


Figure 4: Regional geologic map showing the location of the Candelaria Deposit relative to the coastal batholith and Cretaceous sediments and volcanics. Map modified from Mpodozis and Allmendinger (1982).

Atacama Fault, a major strike-slip system that has been active since at least the middle Jurassic, cuts the batholith along the length of its axis (Brown et al., 1991). Studies of the magmatic and tectonic evolution of the Andean Cordillera (Coria et al., 1982; Mpodozis and Ramos, 1990) indicate that during Early Cretaceous time the area east of the coastal batholith was part of a back arc basin that developed into an "aborted" marginal basin. This was marked by the eruption of calc-alkalic andesitic and basaltic lavas of the Punta del Cobre Formation that underlies carbonates and clastic sediments of the Lower Cretaceous

Chañarcillo Group. These sediments were apparently deposited along a stable continental margin on the narrow shelf of the Aconcagua Platform (Biese, 1942; Segerstrom and Ruiz, 1962; Segerstrom et al., 1963). The center of magmatic activity migrated eastward with the emplacement of the mid-Cretaceous batholith along and to the east of the Atacama Fault Zone (Segerstrom, 1959; Farrar et al., 1970; Zentilli, 1974; Clark et al., 1976; Brook et al., 1986; Brown, 1988). Extensional tectonics continued in the early part of Late Cretaceous time with the formation of a large "aborted" basin that filled with andesitic lavas, conglomerates, pyroclastic breccias, and tuffs of the Cerrillos Formation in the Copiapó area (Segerstrom and Parker, 1959; Mpodozis and Ramos, 1990).

LOCAL GEOLOGY

Volcanic and Sedimentary Rocks

The oldest rocks in the area of the Candelaria Deposit are metavolcanics of the Punta del Cobre Formation of Early Cretaceous age (Segerstrom and Ruiz, 1962; Fig.5). In its type area the formation has been divided into three units (Ortiz et al., 1961) (1) a lower volcanic unit made up of andesitic flows and flow breccias, (2) a sedimentary unit with shales and medium-to coarse-grained volcaniclastic sediments, and (3) an upper volcanic-sedimentary unit with interbedded calcareous shales, poorly sorted breccias and conglomerates with chert fragments, andesitic-lavas, and flow breccias with amygdules.

According to Tilling (1962) and Segerstrom et al. (1963), the Punta del Cobre Formation is conformably overlain by limestones, calcareous argillites, and calcareous sandstones of the Abundancia Formation and their metamorphic equivalents. However, Alfaro (1967) described an angular unconformity between the Punta del Cobre Formation and the overlying Abundancia Formation in the area north of Quebrada Meléndez. Data from drilling and open pit mapping have shown that the contact between the Punta del Cobre and Abundancia Formation is clearly unconformable in the area of the Candelaria Deposit.

The Nantoco Formation conformably overlies the Abundancia Formation and is made up predominantly of medium-bedded grey limestone with a few thin sandstone or calcareous argillite beds east of Candelaria (Segerstrom et al., 1963; Tilling, 1962). At and west of Candelaria the Nantoco Formation has been metamorphosed to a series of garnetites and skarns containing thin, interbedded layers of hornfels (Tilling, 1962).

Intrusive Rocks

Pyroxene diorite and albite soda-granite of a mid-Cretaceous batholith crop out about 1 km west of the Candelaria Deposit (Tilling, 1962; Segerstrom et al., 1963). Tilling (1962) described the pyroxene diorite as a dark grey coarse-grained holocrystalline rock consisting of plagioclase, ferromagnesian minerals, potash feldspar, and minor quartz. The grain size of the constituent minerals averages 6 to 7 mm with some plagioclase laths reaching 2 cm in length. Plagioclase grains are commonly zoned with compositions between An₄₂ and An₂₆. Orthoclase partially or completely rims plagioclase, and myrmekitic borders are common. Orthoclase is also present as slightly perthitic anhedral grains filling interstices. Quartz occupies voids and forms micrographic intergrowths with orthoclase.

Pyroxene and amphibole are the principle mafic minerals; biotite is rare. Pyroxene is diopsidic augite that is present as poikilitic grains that are smaller than plagioclase grains. Pyroxene has commonly been uralitized or altered to green actinolite. Amphibole is present as phenocrysts of strongly pleochroic green hornblende and as reaction rims around pyroxene. Some amphibole has altered to biotite or chlorite. The pyroxene diorite has a gneissic or schistose texture produced by shearing along the contact with the adjacent sedimentary rocks.

The albite soda-granite is described by Tilling (1962) as a fine- to medium-grained leucocratic rock with porphyritic texture. Plagioclase (An_{4-10}) is present both as sericitized subhedral phenocrysts that reach a maximum of 3mm in size and as small laths in the matrix. Some plagioclase of oligoclase or andesine composition is present. Quartz is present as small anhedral grains in the groundmass. When present, orthoclase is also found as small anhedral grains in the matrix. Ferromagnesian minerals are almost totally absent, but amphibole when present occurs as subhedral grains of actinolite that may be of secondary origin.

The contact between these intrusives and Lower Cretaceous sedimentary rocks is marked in places by a wide but discontinuous zone of strong shearing that Tilling (1962) interpreted to have resulted from forceful intrusion of the batholith. Within the shear zone the earlier intrusives, the sheared contact rocks, and the Lower Cretaceous sedimentary rocks are all cut by dikes that range in composition from aplite to basalt.

Contact Metamorphism and Metasomatism

Emplacement of the Andean Batholith into predominantly calcareous Lower Cretaceous rocks of the Chañarcillo Group produced a wide contact-metamorphic and metasomatic aureole that was studied in detail by Tilling (1962). This contact-metamorphic and metasomatic zone extends regionally along the length of the Andean Batholith.

In the area of the Candelaria Deposit the contact aureole is exceptionally broad, attaining a maximum width of 3.5 kms but averaging about 2.5 kms. The contact zone is mainly confined to the west of the Copiapó Valley but locally extends eastward into the Punta del Cobre District. According to Tilling (1962), in the inner 2 kms of the aureole the calcareous and volcanic country rocks have been contact metamorphosed to hornfelses or metasomatized to coarse-grained garnetites and fine- to coarse-grained calc-silicate rocks. The sheared contact zone between sedimentary rocks and batholith has been recrystallized to the extent that the original shearing and foliation now appear as ghosts or color differences in a sugary groundmass. Lenses of garnetite are present within the shear zone, suggesting that shearing may have occurred after formation of some contact-metamorphic and metasomatic rocks and thus after emplacement of the part of the batholith responsible for strong contact metamorphism and metasomatism but before emplacement of the intrusions responsible for the strong recrystallization in the shear zone and other rocks in the area. This could account for the discontinuous nature of the sheared contact, since newer intrusives would have cut and metamorphosed parts of the older shear zone. The limestones nearest the batholith in the outer part of the aureole contain tremolite with minor diopside and garnet (Fig. 5); this assemblage grades outward into recrystallized limestone.

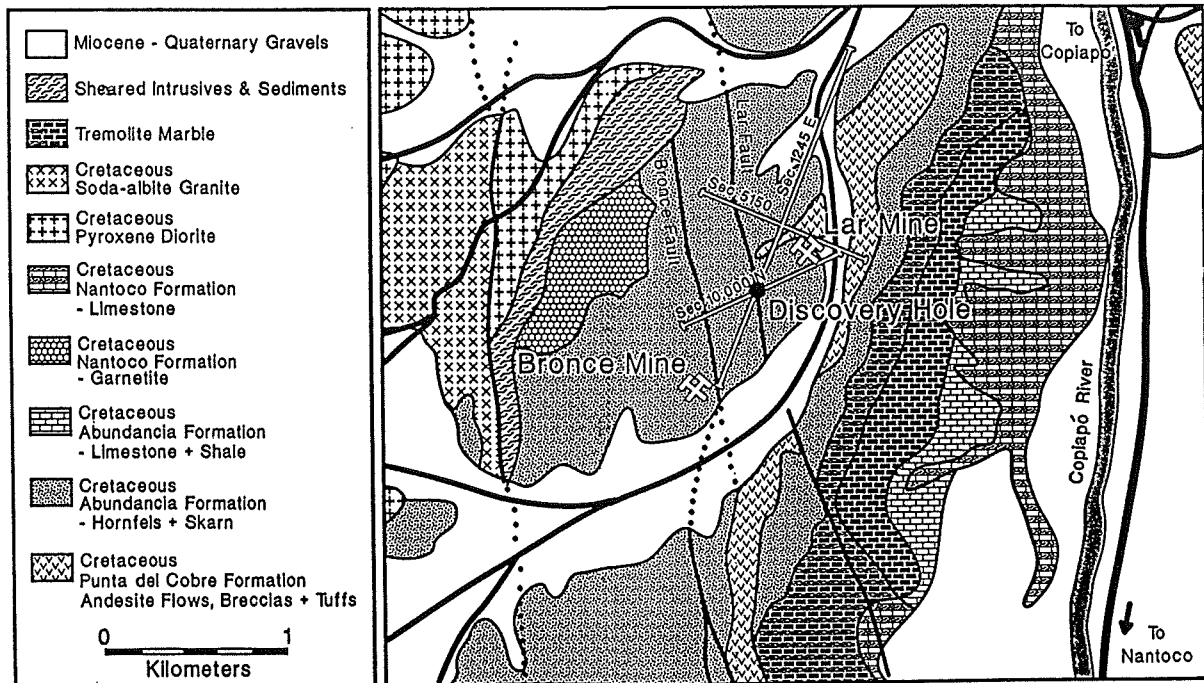


Figure 5: Generalized geologic map of the Candelaria Deposit showing the locations of cross-sections shown in Figures 8, 9, and 10.

Structural Geology

The most prominent structural feature in the region is the shallow-dipping Tierra Amarilla Anticlinorium (Segerstrom, 1960). Recent work done by the Chilean Geological Survey suggests that the anticlinorium may in fact be an antiformal stack of thrust plates (Arévalo and Mpodozis, 1991). The sheared contact between the intrusives of the mid-Cretaceous batholith and Lower Cretaceous sedimentary rocks may be related to this thrusting or may represent an earlier period of faulting.

The Tierra Amarilla Anticlinorium is cut by a series of high-angle faults that can be traced continuously for many kilometers. The trend of these faults has frequency maxima at north-south and N10°W (Tilling, 1962). Other common fault trends are N40 to 50°W and N40 to 50°E. The N40 to 50°W set cuts and offsets the north-south and N10°W fault set, but it is not clear if this is always the case. The observed faults appear to have either normal or high-angle reverse movements. There may have been left-lateral movements of at least 50 to 100 m on some of the N10°W faults and left-lateral movement of 10 to 20 m on the N40 to 50°W faults. All of the high-angle faults appear to be post-mineralization, and most appear to be post-metamorphic.

Stratigraphy

Lower Andesites

The lower andesites consist of a thick sequence of dark grey to brown metamorphosed porphyritic andesite flows, minor crystal tuffs, and volcanic breccias that in many places appear to have been sheared prior to metamorphism. These probably correspond to the

lower andesites of the Punta del Cobre District (Ortíz et al., 1961) and are the main host rocks for the mineralization of the Candelaria Deposit. The total thickness of the lower andesites is unknown but exceeds 600m. The lower andesites typically contain 10 to 20% euhedral 1- to 2-mm plagioclase phenocrysts that have a composition around An₂₅, but many such plagioclase phenocrysts have been partially to completely replaced by orthoclase. The remainder of the rock is made up of 15 to 60% brown magnesium-ferric iron biotite that has formed in the groundmass or has replaced previous mafic minerals, 5 to 15% porphyroblastic hornblende crystals averaging 1 to 2mm long by 0.15mm wide, minor garnet porphyroblasts, and 10 to 15% fine-grained interstitial plagioclase, orthoclase, and quartz. Accessory sphene, epidote, allanite, and recrystallized apatite are common.

The textures of the andesites suggest that they were recrystallized during metamorphism. Biotite commonly mimics earlier shearing that produced gneissic to schistose texture locally. Folded, mineralized quartz veins have been annealed and no longer show strain related to shearing and folding. Shearing and later recrystallization have destroyed earlier volcanic textures in most of the lower andesites. Even in weakly sheared areas the original mafics and fine-grained groundmass in the andesites have been replaced by biotite that has grown parallel to original shear directions, producing a weak foliation.

Retrograde metamorphism has locally produced alteration of plagioclase to albite, epidote, clinozoisite, sericite, and calcite and at least partial conversion of the magnesium-ferric iron biotite to green ferrous iron-aluminium biotite, growth of poikiloblastic hornblende, and partial conversion of biotite and hornblende to chlorite. Locally veinlets of tourmaline, datolite, prehnite, or chabazite and stilbite cut the lower andesites.

Tuffs or Volcaniclastic Sediments

Overlying the lower andesites is a sequence of reworked tuffs or volcaniclastic sediments that have been metamorphosed to hornfels, phyllites, and schists. This unit varies in thickness from 0 to 200m and may correspond to the middle shale and volcaniclastic unit in the Punta del Cobre District (Ortíz et al., 1961). The original nature of these rocks is difficult to determine due to the strong contact-metamorphism, metasomatism, and recrystallization that they have undergone.

The unit is highly variable, characterized in places by prominent banding and in others by breccia horizons. In less mineralized areas relic sedimentary textures can still be seen. Banding in most beds is accentuated by varying amounts of brown magnesium-ferric iron biotite, andraditic garnet, actinolite, amphiboles of the hornblende series ranging in composition from hornblende to ferrohastingsite, diopsidic-hedenbergitic pyroxene, quartz, orthoclase, plagioclase, sodic scapolite, sphene, and recrystallized apatite. In some areas the base of the unit is marked by an unusual horizon of one or more biotite-rich layers with disseminated small euhedral pink garnets followed by a sequence of bedded rocks with coarse crystalloblastic cordierite and prismatic anthophyllite or sprays of fibrous cummingtonite in a matrix of pale brown iron-poor to magnesium-rich biotite, granular orthoclase, plagioclase, and quartz which may be the metamorphic equivalent of a chloritized andesitic tuffaceous or sedimentary horizon.

As in the lower andesites, retrograde metamorphic effects have locally altered plagioclase to albite, epidote, clinozoisite, sericite, and calcite and have partially converted magnesium-ferric iron biotite to ferrous iron-aluminium biotite. Poikiloblastic hornblende has begun to form, and there has been some conversion of hedenbergite to a hornblende near ferrohastingsite in composition. Biotite and hornblende have begun to alter to chlorite and epidote. There appears to be a crude zoning in the unit, with hornblende-ferrohastingsite-rich rocks lower in the section grading upward into increasingly diopside-hedenbergite-rich rocks capped by garnet-scapolite-diopside rocks.

Upper Andesites

The upper andesite unit unconformably overlies the tuffs or volcaniclastic sediments and is locally present as lenses within them. These andesites may be equivalent to the upper volcanic-sedimentary unit of the Punta del Cobre District (Ortíz et al., 1961). The unit is made up of variable thicknesses of massive dark brown to dark green andesite flows with a few discontinuous interbedded volcanic breccia horizons and crystal tuffs. The flows are sometimes amygdaloidal and contain scattered small plagioclase phenocrysts (An_{25-40}). The upper andesite unit ranges from 0 to over 200m thick and is the only part of the Punta del Cobre Formation that crops out in the mine area.

Upper andesite rocks have been metamorphosed to hornfels with plagioclase, biotite, hornblende, orthoclase, and quartz. Plagioclase phenocrysts have become more sodic, and the mafic minerals have been replaced by actinolite or biotite. Near their contact with the overlying sediments the upper andesites are commonly converted to fine- to coarse-grained skarns composed of varying proportions of andraditic garnet, amphiboles ranging from actinolite to hornblende-ferrohastingsite, diopsidic-hedenbergitic pyroxene, sodic plagioclase, sodic scapolite, and quartz with abundant accessory epidote, clinozoisite, sericite, calcite, sphene, recrystallized apatite, and minor allanite and tourmaline. Retrograde alterations are similar to those of the lower andesite and the tuffs or volcaniclastic sediments. No significant mineralization has been found in the upper andesite unit.

Metasedimentary Rocks

The upper andesites are unconformably overlain by skarns and hornfelsed rocks that represent metamorphosed equivalents of the Abundancia and Nantoco Formations. A discontinuous low-angle shear with abundant clay marks the contact between these metasedimentary rocks and the upper andesites in the open pit of the Candelaria Deposit. The metasedimentary rocks vary in thickness from 0 to more than 500m.

The metamorphosed and metasomatized sediments overlying the Candelaria Deposit correspond to the lower "mixed rock" unit of Tilling (1962) and De Neufville (1961). This unit is made up of interbedded hornfels, skarns, and garnetites. The skarns are made up predominantly of varying mixtures of brown andradite garnet (Ad_{68-96} ; Tilling, 1962), green diopsidic to hedenbergitic pyroxene (Hd_{40-82} ; De Neufville, 1961; Tilling, 1962), pale green actinolite, sodic scapolite (Me_{18-30} ; De Neufville, 1961; Tilling, 1962), plagioclase ranging from albite to andesine in composition, quartz, calcite, magnetite, and pyrite. There are a few thin interbedded garnetites that consist of more than 90% andradite garnet; locally these

include examples of a "spotted garnetite" described by Tilling (1962) as containing large zoned garnet porphyroblasts with darker brown cores and lighter brown rims in a matrix of fine-grained light brown garnet. Tilling (1962) has noted that the darker garnets have compositions near Ad_{92} and the lighter rims and matrix have compositions near Ad_{72} . Hornfels is the predominant metasedimentary rock type in the area of the deposit and is composed of differing mixtures of plagioclase (An_{5-53}), biotite, quartz, diopsidic to hedenbergitic pyroxene, pale green actinolite, and sodic scapolite. Scapolite replaces earlier skarn minerals (Tilling, 1962). Hornfels near the base of the section is commonly cut by late actinolite (now partially or totally altered to chlorite)-pyrite veinlets and by potassium feldspar that floods out along fractures and bedding planes and partially replaces scapolite and plagioclase in the hornfels and skarns.

The metasedimentary rocks commonly contain abundant disseminated pyrite and magnetite, especially in the skarns; sodic scapolite-rich skarns contain local layers of massive magnetite with disseminated pyrite. In places the garnet-pyroxene-scapolite skarns are host to small lenses of high-grade magnetite, pyrite and chalcopyrite mineralization such as were mined in the Lar and Bronce Mines.

Intrusive Rocks

The metamorphosed rocks in the Candelaria Deposit have been cut by intrusive dikes, sills, and possibly small stocks. These intrusive rocks include aplite, diabase, dacite, tonalite, and granodiorite. The dacites, tonalites, and granodiorites have been metamorphosed but not sheared. Mafic minerals have been replaced by actinolite, hornblende, or diopside-salite. Plagioclase has become more sodic or been replaced by scapolite, and matrices commonly show growths of new orthoclase. In places these rocks have been cut by garnet veins or partially altered to scapolite skarns. Aplitic dikes and sills are near the batholith and are not present in the mine area. Basaltic and diabasic rocks are post-metamorphic and are present as thin dikes associated with the post-mineralization fault zones. These dikes consist of dark grey-green fine-grained rocks with randomly oriented plagioclase laths, small fresh augite prisms, and abundant bowline after olivine. No intrusive rocks that appear to be a possible source for mineralization were found during the mapping or exploratory drilling.

Quaternary Sediments

The foregoing rock units are partially covered by up to 40m of consolidated late Tertiary terrace gravels and unconsolidated Recent valley gravels in the bottom of the main valley and side washes near Candelaria.

Structural Geology

The Candelaria Deposit is hosted by thermally metamorphosed Lower Cretaceous andesitic volcanics of the Punta del Cobre Formation and to a minor extent by metamorphosed sediments of the Abundancia Formation. The deposit is located near the core of the Tierra Amarilla Anticlinorium, and the metasediments dip 10 to 30° east on the east side of the deposit and 10 to 30° west on the west side of the deposit with locally steeper

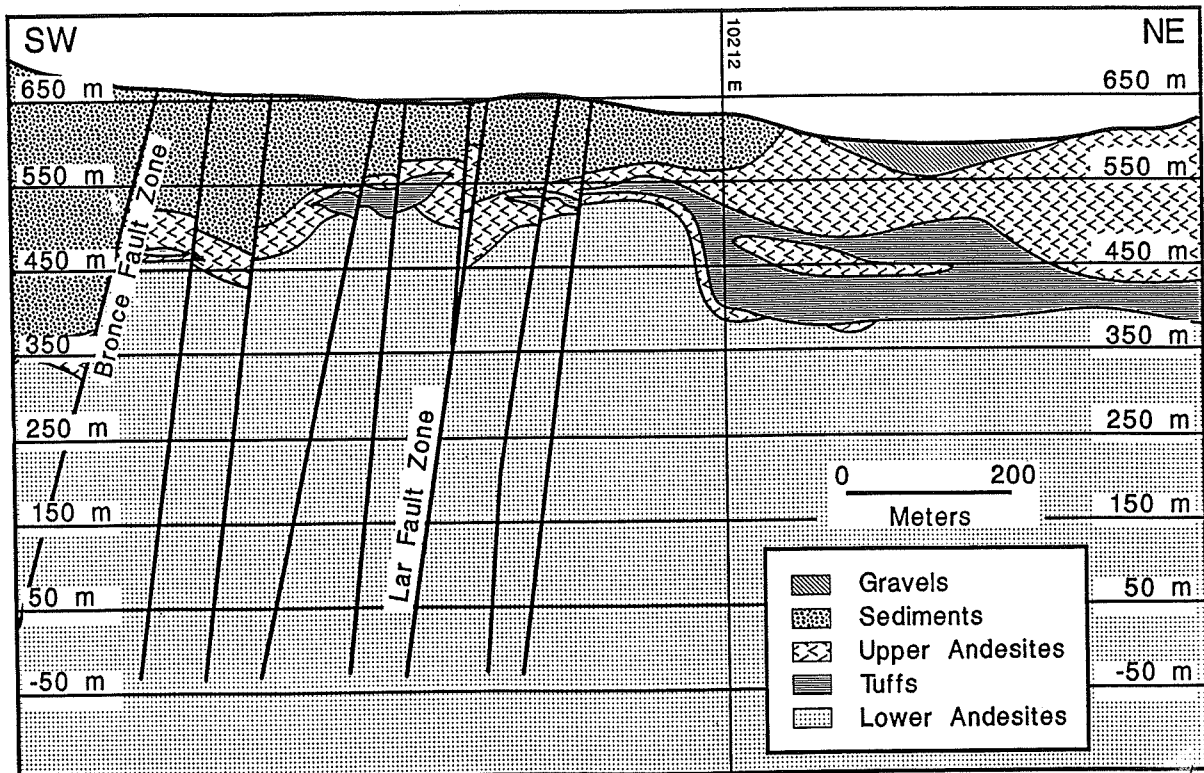


Figure 6: Typical geologic cross-section through the Candelaria Deposit showing the unconformable nature of most of the lithological contacts. Note the steep-sided asymmetrical fold located near the center of the section.

dips near areas cut by later faulting. The structure of the underlying Punta del Cobre Formation is less clear due to the presence of several disconformities and the highly variable thicknesses of the volcanic units (Fig.6). The structure of the Punta del Cobre Formation may be different and unrelated to that of the overlying sediments. In the area of the main orebody the volcaniclastic sediments or tuffs form an asymmetrical structure with an eastern side that dips from near vertical to 60° east and a shallower and now faulted western side that dips 30 to 40° west. The axis of this structure is roughly parallel to the main post-mineralization faults, and the structure appears to close to the north and remain open to the south. Changes in dip in the volcanic units are not reflected in the overlying metasediments, and it is not clear if this is due to extensive deformation of the volcanic units before deposition of the overlying sedimentary rocks or to thrusting of the sedimentary rocks over the underlying volcanics. In either case the sedimentary rocks appear to have been placed on top of the volcanics before contact metamorphism, which has affected both to an equal degree.

All of the rocks in the area have been cut by faults that trend $N10^{\circ}W$, $N40$ to $50^{\circ}W$, and $N40$ to $50^{\circ}E$. Most important of these faults are the $N10^{\circ}W$ -trending Lar and Bronce Faults. The Lar Fault is a high-angle reverse fault that dips about 80° west and has an apparent vertical offset ranging from 35m in the northern part of the deposit to 150m in the southern part of the deposit. The Lar Fault cuts the northern part of the orebody in half and marks the eastern limit of the orebody in the south. In exposures in the west wall of the

open pit there are near-horizontal slickensides that indicate that there has been some left-lateral movement along the Lar Fault. The amount of horizontal movement is unknown, but on some levels the mineralized blocks seem to have been offset by 50 to 100m. Paralleling the Lar Fault 350m to the west is the Bronce Fault, a normal fault that dips 80° west and has a vertical offset of more than 200m, and between these main faults and to the east of the Lar Fault there are several parallel faults that appear to have only minor vertical and horizontal displacements. These minor N10°W-trending faults have been cut and displaced 10 to 20m left-laterally by faults of the N40 to 50°W-trending set. In the area of the main deposit there is a discontinuous N40 to 50°E-trending fault set. These N40 to 50°E-trending faults contain biotite, indicating that they are pre-metamorphic in age.

Surface mapping in the area of the Candelaria Deposit identified one small eastward-verging thrust, and several similar low-angle post-metamorphic faults have been identified in the open pit. These faults have dips that range from 20° to 60° west, one of which is a discontinuous north-south-trending low-angle shear between overlying metasedimentary rocks and underlying metavolcanic rocks. This sheared zone is post-mineralization and post-metamorphic in age.

At depth there is strong development of biotite along foliation planes in the andesitic rocks of the deposit. This has apparently been produced by metamorphism of previously sheared, altered, and mineralized andesitic volcanics and may be related to shearing seen along the contact of the batholith west of the Candelaria Deposit.

MINERALIZATION AND ALTERATION

The ore at Candelaria consists of varying proportions of chalcopyrite, magnetite, pyrite, pyrrhotite, and sphalerite in a gangue of biotite, calc-silicates, and potassium feldspar. Mineralization is present in all the stratigraphic units described except the intrusive rocks, but most of the mineralization is in the lower andesite; the highest grade mineralization is in the overlying volcaniclastic sediments or tuffs. Only minor non-economic mineralization is present in the upper andesites, and mineralization in the metasediments is confined to a few small isolated mantos such as those originally mined in the Lar and Bronce Deposits. Copper mineralization is present in the Candelaria Deposit as fine to coarse disseminations, and as chalcopyrite in veins, breccia fillings, irregular pods, or stringers along foliation planes. Gold is present principally as micron-size grains associated with chalcopyrite or in fractures in pyrite.

Ore Mineralogy

A mineralogical study was undertaken as part of the metallurgical and geological feasibility study (Dufek and Wright, 1989) and later investigations (Williams, 1990, 1994).

Magnetite

Magnetite is common in the ore body and makes up about 10 to 15% of the ore. It is generally in euhedral grains that average about 0.2 mm in diameter. It occurs in folded and sheared veins, unfolded veins, stringers, sheared and unsheared breccias, massive to

semi-massive lenses and pods, disseminations in wall rocks, and as euhedral to anhedral inclusions in chalcopyrite, pyrite, pyrrhotite, and sphalerite. Grain size sometimes coarsens along contacts with chalcopyrite and pyrite, indicating possible formation or recrystallization of magnetite with sulfides. Magnetite is also commonly intergrown with silicates and has developed along cleavage planes in amphiboles, formed as interstitial grains between silicate minerals, and replaced earlier amphiboles and biotite. In some places it has formed skeletal crystals that show progressive growth in chlorite that has replaced hornblende. There are long narrow grains of magnetite that appear to have replaced hematite or amphibole or other silicates. Magnetite has also formed from the breakdown of pyrrhotite, where it has produced pseudomorphic myrmekitic-like intergrowths with pyrite and marcasite that are locally replaced by chalcopyrite.

There may have been more than one period of magnetite formation. Magnetite appears to predate the copper mineralization and may be related in part to contact metamorphism and associated iron metasomatism. Some euhedral magnetite grains show zonal growth indicative of initial magnetite being overgrown by later stage magnetite. Magnetite is present in veins and breccias where it has been sheared and stretched before metamorphism and also in cross-cutting undeformed breccias that appear to have formed during or after the later stages of contact metamorphism and iron metasomatism. Because of the effects of contact metamorphism and iron metasomatism, it is difficult to tell if the latter period of magnetite formation represents a second influx of magnetite mineralization or a remobilization of earlier mineralization.

Pyrite

Three stages of pyrite mineralization have been recognized. Pyrite I is primary and generally forms euhedral crystals or amoeboid porphyroblasts with sieve texture involving abundant inclusions of silicate minerals. It occurs in folded and sheared veins, unfolded veins, stringers, sheared and unsheared breccias, foliation planes, irregular pods, and as euhedral grains disseminated in wall rocks. It is the most common type of pyrite in the deposit and is normally associated with chalcopyrite, magnetite, or pyrrhotite, but it also occurs alone in thick veins associated with chlorite. Average grain size is around 0,35 mm, but euhedral crystals reach 3 cms in size. Pyrite I shows the greatest amount of replacement by chalcopyrite of all the opaque minerals probably formed during the late stages of contact metamorphism and iron metasomatism. It is commonly strongly fractured.

Pyrite II formed in association with marcasite and magnetite as an alteration of pyrrhotite. It has an average grain size of 0,08mm and a distinct pseudomorphic texture in which the octahedral (111) face of pyrite II coincides with the (0001) plane of pyrrhotite. Pyrite II apparently formed during the late stages of contact metamorphism and iron metasomatism, probably as a result of changes in oxidation potential (Picot and Johan, 1982).

Pyrite III typically forms thin veinlets cutting chalcopyrite and has an average grain size of around 0,04 mm. It appears to have formed late in the history of the deposit.

Chalcopyrite

Chalcopyrite is the only copper mineral of importance in the Candelaria Deposit, where it has a relatively coarse grain size averaging around 0,5mm. It is found in both folded and unfolded veins, sheared and unsheared breccias, along foliation planes, as almost massive irregular pods and patches, in tension fractures, and as fine to coarse disseminations. It also occurs as irregular to rounded inclusions in pyrite, pyrrhotite, magnetite, and sphalerite. It commonly forms complex intergrowths around or filling fractures and cleavage planes in silicates such as hornblende, actinolite, biotite, pyroxene, and to a lesser extent, quartz, orthoclase, chlorite, epidote, plagioclase, clinozoisite, and garnet. Chalcopyrite has extensively replaced opaque minerals, especially pyrite and pyrrhotite and to some extent magnetite. The boundaries between chalcopyrite and other opaque minerals are simple, with linear or gently curving boundaries being typical, but complex intergrowths with magnetite in which chalcopyrite has partially or wholly replaced original pyrite in myrmekitic pyrite-magnetite intergrowths have developed.

Gold

Gold is present mainly as micron-sized grains associated with chalcopyrite, especially where the chalcopyrite has replaced pyrite I or pyrite II, but is also present to a lesser degree in fractures cutting pyrite I. There is also gold in the pyrite, either in embayments and veinlets with chalcopyrite or in fractures or along grain boundaries that are part of grains that are partially replaced by chalcopyrite. Gold has also been found as blebs in pyrite I with no associated chalcopyrite, but such occurrences without chalcopyrite are rare. Dufek (1989) found that the gold grains included in pyrite I had the highest gold content and the least amount of silver (96,5 to 99,9 gold) while gold grains found along grain boundaries and fractures in pyrite I and II and in chalcopyrite veinlets cutting pyrite I and II contain lesser gold and higher silver (92,4 to 96,3 gold). The lowest gold and highest silver contents (77,7 to 91,0 gold) are in gold grains associated with chalcopyrite and chalcopyrite embayments in pyrite I and II.

Pyrrhotite

Pyrrhotite forms anhedral granular aggregates in veins, pods, stringers, and disseminations. It is also present as replacement remnants in chalcopyrite and as inclusions in magnetite, arsenopyrite, and pyrite I. Pyrrhotite has an average grain size of around 0.2 mm and is most common in the tuffs or volcaniclastic rocks but is also present in the lower andesite. It forms complex intergrowths with silicate minerals, especially hornblende. In two of the samples studied pyrrhotite under crossed polarizers shows lamellae that probably formed by exsolution of a two-phase mixture (Uytenboggardt and Burke, 1971). Pyrrhotite has commonly been partially or totally replaced by mixtures of pyrite II, marcasite and magnetite; the pseudomorphic texture produced shows the octahedral (111) faces of pyrite II and magnetite oriented parallel to the (0001) planes of the original pyrrhotite grains. Marcasite is also commonly oriented in linear strings of grain-aggregates parallel to the (0001) planes in the original pyrrhotite. These replacements may have resulted from changes of oxidation potential (Picot and Johan, 1982) that occurred during late stage metamorphism and iron metasomatism.

Marcasite

Marcasite has formed along with pyrite II and magnetite as an alteration product of pyrrhotite and is most frequently present as lamellar to irregular grain-aggregates aligned parallel to the (0001) planes of pyrrhotite. Because of the almost total replacement of pyrite II and marcasite by chalcopyrite, fine linear grains of marcasite in chalcopyrite are the only evidence of the former existence of pyrrhotite. Because marcasite is a product of late alteration of pyrrhotite, it has not generally developed the complex intergrowths with silicates seen with other opaque minerals. Marcasite has an average grain size of approximately 0,07mm.

Sphalerite

Sphalerite is generally a minor phase in the deposit, but it is widely distributed and may make up more than 10% of the ore minerals in some areas. It is present in aggregates of reddish brown anhedral grains with an average size of around 0,1mm. Dufek (1989) checked a few isolated grains not associated with pyrrhotite with a scanning electron microscope and found that they contained between 2 and 5% iron. Sphalerite forms intergrowths with chalcopyrite, pyrrhotite, pyrite, galena, magnetite, and pyrrhotite and its alteration products. It may form as "star" inclusions in chalcopyrite and may also contain exsolved blebs of chalcopyrite oriented along crystallographic planes. Sphalerite also forms intergrowths with chlorite and has been found with galena in veinlets cutting garnet.

Galena

Galena is a minor phase in the deposit and is usually associated with sphalerite, but it may also be intergrown with chalcopyrite and silicate minerals. It forms euhedral to anhedral grains averaging 0,04 mm in size.

Hematite

Both primary and secondary hematite occur in the deposit. Primary hematite is present as acicular needles in silicate gangue and as fine intergrowths along cleavages in hornblende and biotite. Secondary hematite occurs as an alteration product along octahedral planes, microfractures, and grain boundaries in magnetite (martitization) and has also been found as veinlets cutting chalcopyrite and the alteration products of pyrrhotite, where it replaces magnetite grains from the outside inwards. In some samples magnetite has replaced the acicular form of hematite. Magnetite replacement of hematite is suggested by long narrow magnetite grains that contain fine linear inclusions of hematite and by magnetite crystals with basal cross sections typical of hematite. These pseudomorphs are most commonly intergrown with pyrite I or gangue minerals. Hematite grains average 0,03mm in size.

Ilmenite

Ilmenite is uncommon in the deposit but is present in stringers and veins in gangue and as rounded grain-aggregates with an average grain size of 0,05mm. It is also present

as laths and irregular intergrowths with magnetite. It contains blebs of pyrrhotite and has been replaced by chalcopyrite locally.

Cubanite

Cubanite is present in trace amounts and has an average grain size of 0,07mm. It forms irregular granular aggregates in chalcopyrite, especially along grain contacts with gangue minerals. In some samples orthorhombic cubanite has altered to the cubic variety.

Arsenopyrite

Arsenopyrite is rare in the deposit but is present in euhedral grains, stringers, and veins with an average grain size of about 0,2mm. It is associated with and commonly contains inclusions of pyrrhotite and its alteration products. In a few cases chalcopyrite has replaced arsenopyrite.

Molybdenite

Molybdenite is present in only a few samples, where it occurs as grains averaging 0,25mm in size associated with pyrrhotite, pyrite II, chalcopyrite, calc-silicates, and biotite. It appears to be the same age as pyrrhotite.

Anhydrite and Gypsum

Purple to white anhydrite is present in breccia fillings and large veins which cut earlier mineralization and alteration. Anhydrite is typically coarse-grained and may be partially to completely altered to gypsum. The breccias are generally barren, but the veins contain pyrite or chalcopyrite locally.

Paragenesis of Opaque Minerals

Figure 7 presents the paragenetic sequence for opaque minerals in the deposit. Because of the complexity of events, this sequence reflects the assemblages remaining after the last period of metamorphism and remobilization and not the original paragenetic sequence.

Orebodies

The Candelaria Orebodies are sheet-like in form with the main part of the deposit approximately 2 000m long by 600m wide and elongated north-south. In the area of the folded tuffs and volcaniclastic sedimentary rocks mineralization reaches thicknesses of more than 350m and is open at depth (Fig. 8). The steep eastern flank of this structure contains the highest grade mineralization in the deposit. This mineralization is concentrated in the volcaniclastic sedimentary rocks or tuffs and the adjacent underlying lower andesites. Away from the high-grade center and especially to the north, mineralization thins out into several 10- to 50-m thick, manto-like bodies that are roughly controlled by the contact between the volcaniclastic sedimentary rocks or tuffs and the underlying lower andesites. Mineralization

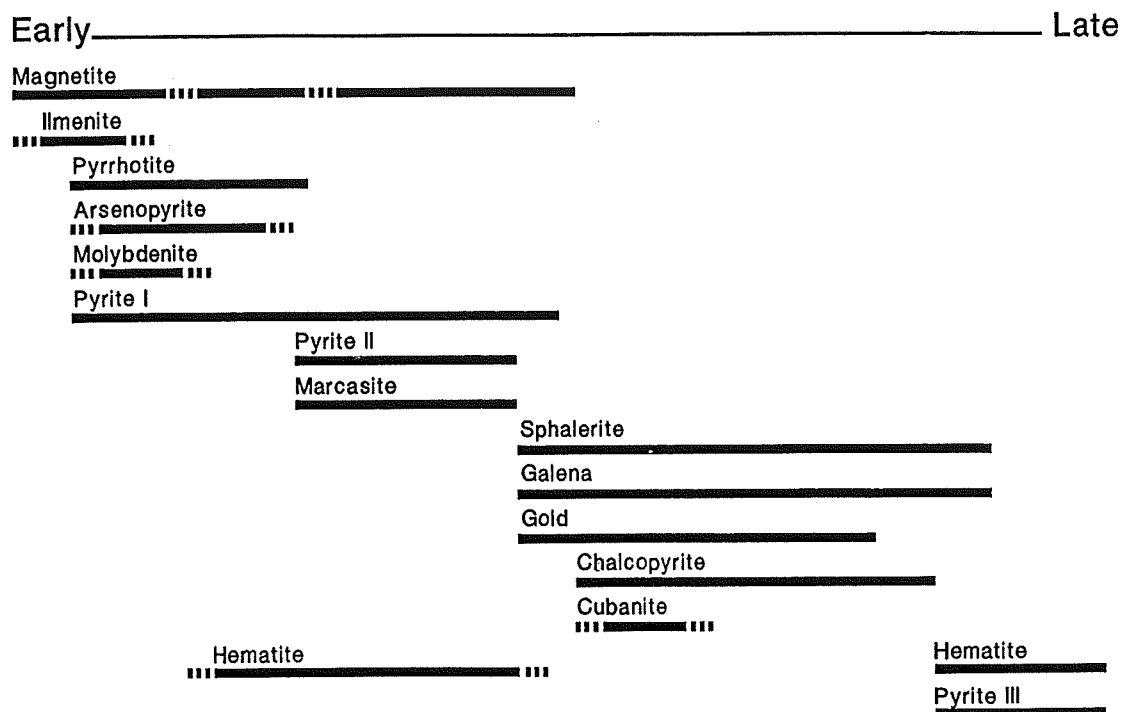


Figure 7: Paragenesis of opaque minerals at Candelaria.

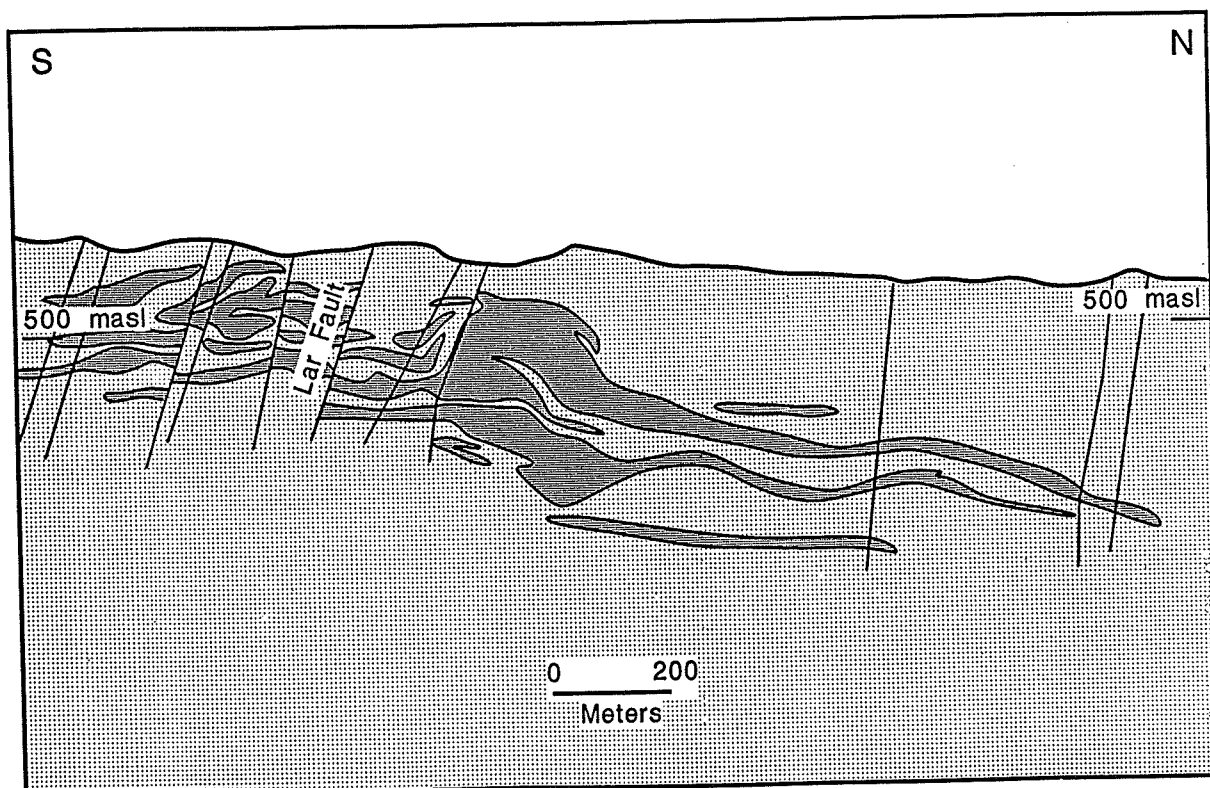


Figure 8: Generalized longitudinal section (1245E) showing the distribution of ore-grade mineralization in the Candelaria Deposit. See Figure 5 for location.

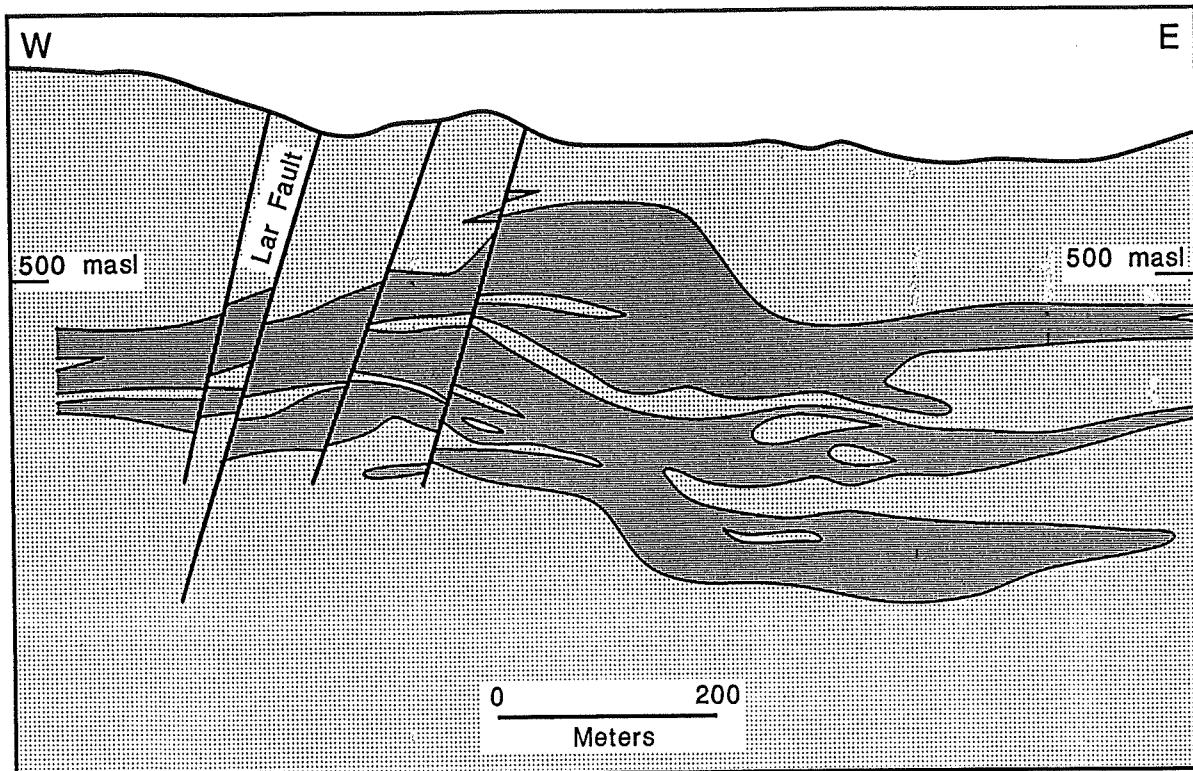


Figure 9: Generalized cross-section (5150) showing the distribution of ore-grade mineralization in the Candelaria Deposit. See Figure 5 for location.

has been cut by a series of high-angle normal and reverse faults. The most important of these are the Lar and Bronce Fault Systems; in some areas these structures have significantly offset the mineralization and limited the amount of ore that can be mined in an open pit.

Gold mineralization appears to be vertically zoned, with higher gold/copper ratios present at the top of the deposit in the skarned metasedimentary rocks and volcaniclastic sedimentary rocks or tuffs than in the lower biotitized andesites.

Magnetite is ubiquitous in the Candelaria Deposit, but there does not appear to be a direct relation between the extent of magnetite mineralization and copper or gold grades. There is a concentration of magnetite in skarns formed in the folded tuffs and volcaniclastic sedimentary rocks and lower andesites immediately below these skarns, and this magnetite concentration is spatially associated with some of the highest grade mineralization in the deposit. However, below this in the lower andesites there is another large magnetite concentration associated with lower grade copper mineralization and abundant magnetite is associated with copper and gold contents well below ore grade in other areas. This may be explained by two distinct periods of magnetite deposition or deposition and remobilization with one more closely associated with mineralization than the other.

Ore Types

Preliminary metallurgical test work defined the following five distinct megascopically observable ore types: (1) skarn ore, (2) pyrrhotite ore, (3) magnetite ore, (4) potassium feldspar ore, and (5) biotite ore. Figure 10 shows the typical cross-sectional distribution of these ore types in the Candelaria Deposit.

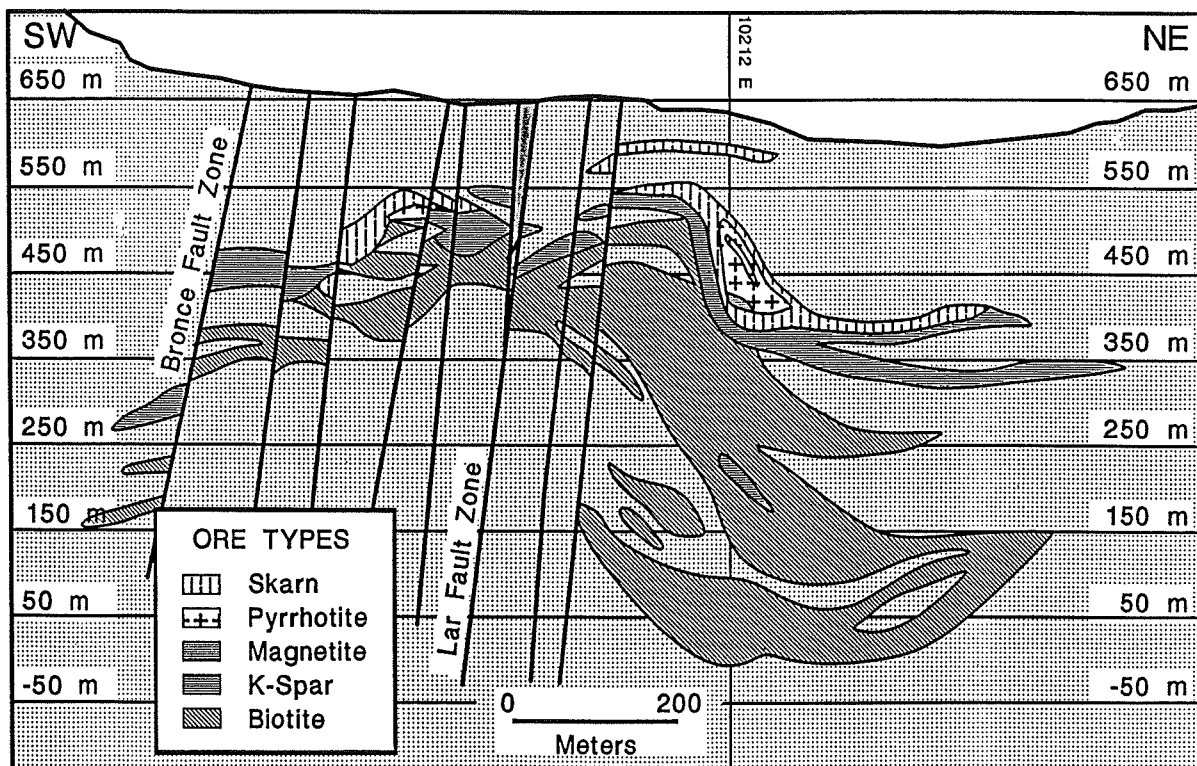


Figure 10: Cross-section 10 000 N showing the typical distribution of various ore types in the Candelaria Deposit. Note that the thickest part of the mineralization occurs below the steep flank of the asymmetric fold. See Figure 5 for location.

Skarn ore consists of ore minerals in a gangue composed of varying mixtures of diopsidic-hedenbergitic pyroxene, andraditic garnet, calcite, quartz, actinolite, hornblende-ferrohastingsite, and sodic scapolite. This ore type has a high density, is hard and abrasive, and makes up approximately 10% of the total ore of the deposit. Metallic minerals occur in fracture fillings, veins, and disseminations following bedding planes. Skarn ore is concentrated near the top of the ore body in the metasedimentary rocks and the upper part of the metamorphosed tuffs or volcaniclastic sedimentary rocks.

Pyrrhotite ore is similar to skarn ore except that pyrrhotite is visibly present. It is most commonly present in the metamorphosed tuffs or volcaniclastic sedimentary rocks but is also present in the lower andesites. Pyrrhotite ore makes up 5% of the ore of the deposit.

The potassium feldspar ore is characterized by the presence of abundant fine-grained pink orthoclase that floods the rock or is present in veins and vein selvages. This ore is usually present along the contact between the metamorphosed tuffs and the metamorphosed

lower andesites and may be superimposed on any of the other ore types. Potassium feldspar ore usually has moderate hardness and density and makes up about 10% of the total ore of the deposit.

Magnetite ore is present as small lenses and pods throughout the deposit and is defined by the presence of more than 50% massive magnetite in lenses, disseminations, or breccia-fillings. It is extremely dense and has moderate to high hardness. Magnetite ore makes up only 3% of the deposit, but significant amounts of magnetite-rich mineralization are present in areas below economic copper cut-off grade.

Biotite ore is found almost exclusively in the lower metamorphosed andesites and makes up nearly 72% of the total orebody. As its name implies, it is characterized by the presence of abundant biotite. It is the least dense and the softest of the ore types.

Alteration

No clear alteration zoning directly associated with the Candelaria mineralization has been identified. This may be due to the combined effects of metasomatism, shearing, one or more periods of contact metamorphism, and retrograde metamorphism. An early period of potassium metasomatism probably accompanied mineralization and added the unusually high content of potassium (3 to 9% K₂O) that has produced abundant magnesium-ferric iron biotite and potassium feldspar in the metamorphosed lower andesites.

Early potassium metasomatism was followed by a later period of sodium metasomatism in which scapolite replaced earlier skarn minerals and plagioclase. Hornblende and hedenbergite also formed at this time. This sodium metasomatism was accompanied by remobilization or new deposition of magnetite, sulfides, and gold.

A second period of potassium metasomatism followed and overlapped retrograde metamorphism. This late and largely post-mineralization period of potassium metasomatism produced strong potassium feldspar flooding along the contact between the tuffs or volcaniclastic sedimentary rocks and upper andesites. Brecciation appears to have been associated with this potassium metasomatism in the most intensely altered areas. Breccia fragments have been largely replaced by potassium feldspar, and original volcanic textures or earlier skarn textures have been largely destroyed. In less severely altered areas potassium feldspar forms wide halos around stockwork-like quartz-potassium feldspar-amphibole ± magnetite ± sulfide veins or replaces feldspar phenocrysts or the matrix in the volcanics. Potassium feldspar flooding extends locally downwards into the lower andesites and upwards into the overlying metasediments along fractures and bedding planes and replaces or cuts earlier formed feldspars, biotite, sodium scapolite, and andraditic garnets. This potassium feldspar alteration is associated with retrograde metamorphic minerals and mineralization locally suggesting that it overlapped retrograde metamorphism. In some areas there seems to be an association of this late potassium feldspar alteration with late cross-cutting and largely barren magnetite breccias and veins. The vast majority of this late potassium feldspar, however, appears unrelated to mineralization and simply overprints the pre-existing metamorphic rocks.

Skarns

The skarn mineralogy in the rocks hosting the Candelaria Deposit does not fit easily into any of the major classes of skarn deposits described by Einaudi et al. (1981), Einaudi (1982), or Meinert (1983, 1989). Chemical analyses have not been done on the skarn minerals, and compositions were determined optically or in the case of the garnets by a combination of optical and X-ray determined cell dimensions. These methods were sufficiently accurate to show the general trends and classifications among the skarn minerals. The wide variety and compositional ranges of pyroxenes and amphiboles, limited range of observed garnet compositions, and abundance of late scapolite suggest a complex history in the development of the skarn mineralogy.

Garnet compositions reported by Tilling (1962) (Ad_{68-96}) were determined on garnets from the metasedimentary rocks which overlie the main mineralization. More aluminous compositions are from lighter coloured rims surrounding more andraditic cores in zoned crystals of some skarn layers. Megascopically the garnets associated with the mineralization have the same appearance as those in the overlying metasediments. Scanning electron microscope analysis (Dufek, 1989) on garnet from a garnet-rich mineralized skarn near the top of the metamorphosed tuffs or volcaniclastic sedimentary rocks indicated a composition well within and to the andraditic end of the garnet compositions reported by Tilling (1962). The garnets studied to date (Fig. 11) fall well within the range for garnets associated with copper, calcic-iron, lead-zinc, and gold skarns (Fig. 12) (Einaudi and Burt, 1982; Meinert, 1989).

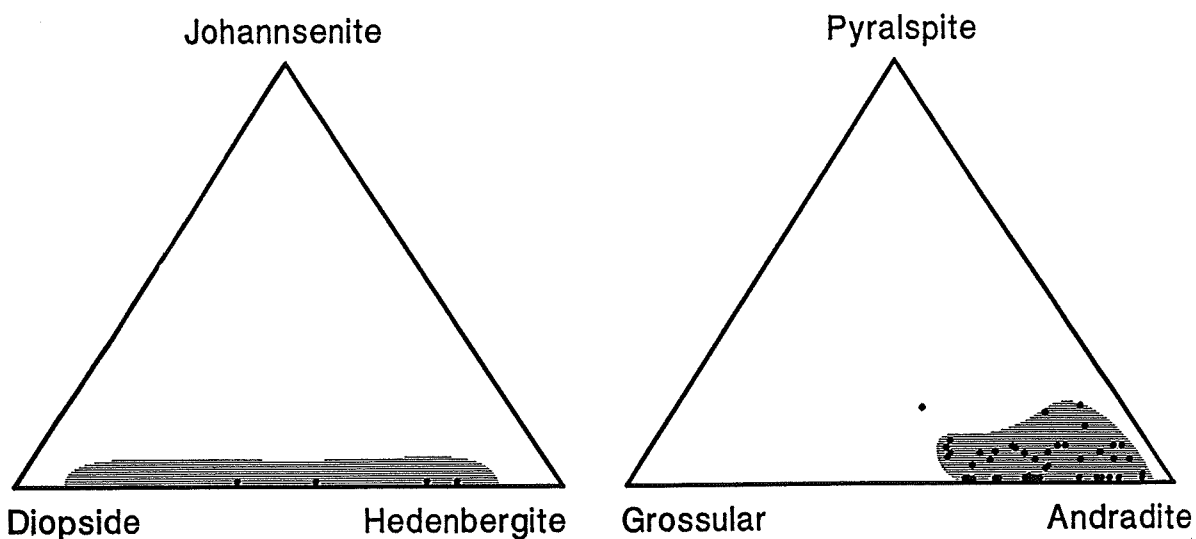


Figure 11: Diagrams showing general compositions of garnets and pyroxenes from the skarns surrounding the Candelaria Deposit. Points are for compositions determined using X-ray diffraction or refractive indices, while the shaded area represents compositions reported in petrographic studies. Data from De Neufville (1961), Tilling (1962), and Williams (1990, 1994).

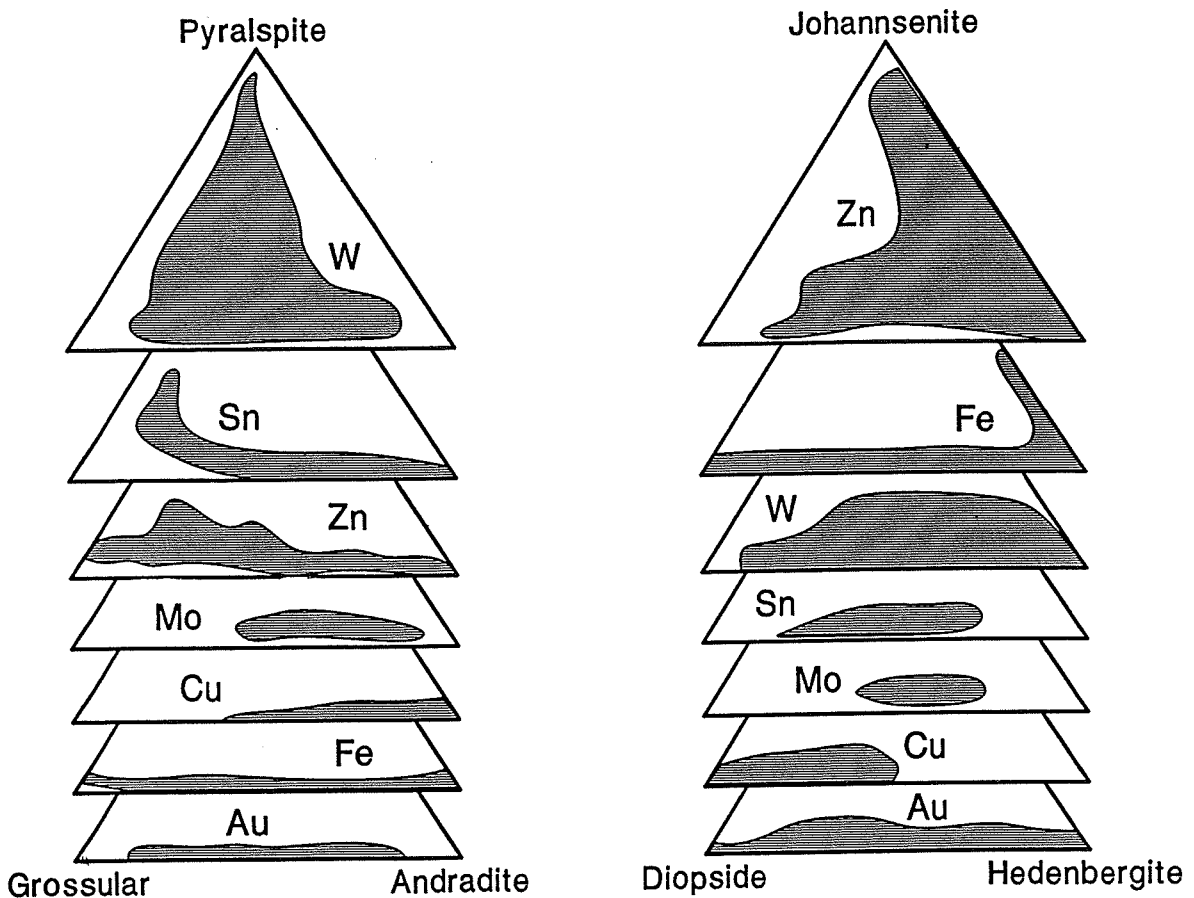


Figure 12: Diagrams showing the general range of garnet and pyroxene compositions of various types of skarn deposits. Modified from Meinert (1983) and Ettlinger et al. (1992).

Green diopsidic to hedenbergitic pyroxene (Hd_{40-82}) such as that reported by De Neufville (1961) and Tilling (1962) was obtained from metasedimentary rocks overlying the mineralization. Optical determinations on other pyroxenes in mineralized rocks varied from diopside to hedenbergite, usually with minor sodium-iron substitution for calcium-magnesium-iron depending on the associated ore mineralogy. In skarns formed in the metamorphosed tuffs or volcaniclastic rocks, pyrrhotite-chalcopyrite-pyrite-magnetite is a common ore mineral assemblage. Here the stable clinopyroxene is hedenbergite. As suggested by Einaudi (1982), this hedenbergite indicates deposition at an oxidation state below the magnetite-pyrite-pyrrhotite buffer. The iron-rich clinopyroxenes (Fig. 11) fall within the range of clinopyroxenes from reduced calcic-iron and gold skarns but outside the range of most clinopyroxenes from oxidized copper skarns (Fig. 12; Einaudi et al., 1981; Einaudi, 1982a, 1982b; Einaudi and Burt, 1982; Meinert, 1983, 1984, 1988, 1989; Myers, 1990). Sodic scapolites are also more typical of iron and gold skarns than of other skarn types (Meinert, 1983, 1988, 1989; Ettlinger et al., 1992). The cordierite-quartz-anthophyllite-cummingtonite-biotite assemblage from the base of the metamorphosed tuffs or volcaniclastic sedimentary rocks does not fit into the normal mineralized skarn classifications but has been reported from regionally metamorphosed sulfide deposits (Kelly, 1975; Riverin and Hodgson, 1980; Sarkar et al., 1980; Elliot-Meadows and Appleyard, 1991).

Stages of Skarn Development

The authors infer an early period of andradite-diopside skarn formation and associated hornfels development under relatively oxidizing conditions similar to those found in copper skarns (Meinert, 1983, 1984, 1988, 1989; Einaudi et al., 1981; Einaudi, 1982a, 1982b; Einaudi and Burt, 1982). This was followed by a later stage of hedenbergite-andradite-scapolite-hornblende skarn formed under more reducing conditions similar to those associated with some calcic-iron and gold skarns (Meinert, 1983, 1983, 1988, 1989; Ettlinger et al., 1992). The presence of abundant sodic scapolites indicates that there was an influx of chlorine and possibly sodium into the system. Burnham (1979) has shown that chlorine is strongly partitioned into the aqueous magmatic phase during the later stages of crystallization of granitic magmas. Studies by Chou and Eugster (1976) and Eugster (1986) suggest that NaCl-rich fluids are capable of remobilizing sufficient iron and copper to account for the formation of the late magnetite breccias and the remobilization of copper at Candelaria. Increase in NaCl may also have caused breakdown and replacement of plagioclase by sodic scapolite with release of aluminium, which then became available to form aluminium-iron amphiboles and the late pale brown aluminium-rich garnets. Increased sodium and iron also produced a shift toward albite in surviving plagioclase compositions, minor substitution of sodium in clinopyroxenes, and formation of hedenbergite and iron-sodium-aluminium-rich amphiboles in association with pyrrhotite.

Deposit Origin

No igneous source has been located for the mineralization of the Candelaria Deposit. The large size of the deposit, its widespread mineralization and spatially associated early potassic alteration, its simple mineralogy, its limited suite of contained metals, and its abundant recrystallized apatite suggest that the original mineralization may have been related to a relatively deep-seated porphyry system emplaced in a pile of andesitic volcanics which were comagmatic with early phases of the adjacent batholith. The lack of a recognizable intrusive source, the flat manto-like shape of part of the ore body, and the abundance of magnetite are all atypical of porphyry copper deposits. The metamorphism and metasomatism that followed the initial mineralization may have destroyed much of the direct evidence related to the origin of the mineralization.

CONCLUSIONS

Based on a combination of field observations and petrographic studies, the following history is suggested for the Candelaria Deposit: An initial period of relatively deep-seated mineralization and associated widespread potassium metasomatism was followed by shearing. This was followed by contact metamorphism and iron metasomatism under relatively oxidizing conditions that formed biotite-plagioclase hornfels, andraditic garnet-diopsidic clinopyroxene skarns in metasedimentary rocks and andesites, and abundant magnesium-ferric iron biotite. The adjacent batholith continued to cool, and metasomatic solutions became richer in halogens. Influx of chloride-rich metasomatic fluids led to the formation of new skarn with garnet, hedenbergite (usually with minor sodium-iron substitution for calcium-magnesium-iron), pyrrhotite, magnetite, iron-sodium hornblendes, albite, and abundant sodic scapolite after contact-metamorphic and iron metasomatic minerals. This new skarn formed

mainly in areas which had previously contained abundant plagioclase. The formation of the scapolite-rich skarns may have been accompanied by a second period of magnetite deposition or may only have remobilized earlier-deposited magnetite. In either case, iron was mobile at this time. Gold may also have been partially remobilized at this time, accounting for the higher gold/copper ratios in the skarns in the upper part of the deposit. Pyrrhotite formed as the stable phase associated with hedenbergite in areas rich in sulfides within the upper skarns, indicating more reducing conditions. Chalcopyrite and other ore minerals were also partially remobilized during this stage and may have concentrated and moved out along the impermeable contact between the older skarns and the underlying volcanics. Retrograde metamorphism with the formation of chlorite, epidote, allanite, actinolite, clinozoisite, and some hornblende followed. Early in this retrograde metamorphism chalcopyrite replaced many of the earlier opaque minerals and pyrrhotite began to break down to pyrite, marcasite, and magnetite. Mineralization continued at a steadily decreasing rate throughout retrograde metamorphism. During the last stages of retrograde metamorphism there was a second period of potassium metasomatism which produced potassium feldspar flooding. The exact source of this metasomatic event is not clear, but it may have been produced by the intrusion of another batholithic phase and associated thermal breakdown of some of the earlier biotite to form potassium feldspar and magnetite. This would also account for the common association of late magnetite-pyrite breccias and veins with the potassium feldspar flooding.

ACKNOWLEDGEMENTS

The authors would like to thank Phelps Dodge Mining Company for providing the time and resources necessary to develop this paper and for permission to publish it. Critical reviews by and discussions with A.H. Clark, G.L. Myers, and S.A. Williams contributed significantly to the paper. Special thanks are given to the exploration staff and the Candelaria Mine Geological Department, whose work and dedication have contributed to the current understanding of the Candelaria Deposit.

REFERENCES

- Alfaro, J.G. 1967. Geología y yacimientos metalíferos del área de Punta del Cobre entre Tierra Amarilla y Quebrada Meléndez. Memoria para optar al título de geólogo. Santiago, Chile. Universidad de Chile, 120p.
- Arévalo, C., and Mpodozis, C. 1991. Tectónica del Grupo Chañarcillo; una franja de cabalgamientos con vergencia al este en el valle del Río Copiapó, Región de Atacama, Chile: Viña del Mar, Chile. Congreso Geológico Chileno, n.6. Actas, v.1 p. 81-83.
- Biese, N. 1942. Distribución del Cretceo Inferior al Sur de Copiapó: Anual del Primer Congreso Pan Americano de Ingeniería de Minas y Geología, I parte, Instituto Geográfico Militar, Santiago, Chile, p.429-466.
- Brook, M., Pankhurst, R., Shepard, T., Shapiro, B. 1986. Andachron; Andean geochronology and metallogenesis: London, Overseas Development Administration. Open-File Report, 83p.

- Brown, M. 1987. The granites of the Coastal Cordillera, northern Atacama Region, Chile. *TERRA cognita*, v.7, p.277.
- Brown, M. 1988. Geochemistry of the granitic complexes, 26-27°S, northern Chile; Santiago, Congreso, Geológico Chileno, 5th, 1988. Actas, p. 1153-1166.
- Brown, M., Dallmeyer, R.D., Diaz, F. and Grocott, J. 1991. Displacement history and tectonic significance of the Atacama fault system (El Salado-Segment), N Chile; $^{40}\text{Ar}^{39}\text{Ar}$ mineral age constraints (abs.): AGU-MSA 1991 Spring Meeting, Eos, Transactions, American Geophysical Union, Baltimore, MD, May 28-31, 1991, v.72, n.17, p.263.
- Burnham, C.W. 1979. Magmas and hydrothermal fluids, In: Barnes, H.L. ed., *Geochemistry of hydrothermal ore deposits*. New York, Wiley-Interscience Publications, John Wiley & Sons, p.71-136.
- Chou, I.-M. and Eugster, H.P. 1976. Solubility of magnetite in supercritical chloride solutions (abs.): Geological Society of American Abstracts with Programs, v.8, n.6, p.811-812
- Clark, A.H., Farrar, E., Calles, J.C., Haynes, S.J., Lortie, R.B., McBride, S.L., Quirt, G.S., Robertson, R.C.R. and Zentilli, M. 1976. Longitudinal variations in the metallogenetic evolution of the Central Andes: a progress report: Geological Association of Canada Special Paper No. 14, p. 23-58.
- Coria, B., Davidson, J., Mpodozis, C. and Ramos, V.A. 1982. Tectonic and magmatic evolution of the Andes of northern Argentina and Chile: Earth-Science Reviews, v.18, p.303-332.
- De Neufville, J. 1961. Stratigraphy, batholith emplacement, and contact metasomatism at Cerro Tierra Amarilla, near Copiapo, Atacama Province, Chile: Yale University, unpublished dissertation presented to the Faculty of the Scholars of the House Program, 143p.
- Dufek, L. 1989. A scanning electron microscopy study of native gold grains at the Candelaria Copper Deposit, Chile: Phelps Dodge Mining Co. Chile, internal report, 10p.
- Dufek, L. and Wright, E. 1989. Mineralogy of the Candelaria Copper Deposit, Chile: Phelps Dodge Mining Co. Chile, internal report, 34p.
- Einaudi, M.T. 1982a. Descriptions of skarns associated with porphyry copper plutons, Southwestern North America, In: Titley, S.R., ed., *Advances in geology of the porphyry copper deposits, Southwestern North America*: Tucson, University of Arizona Press, p.139-184.

- Einaudi, M.T. 1982b. General features and origin of skarns associated with porphyry copper plutons, Southwestern North America, *In:* Titley, S.R., ed., Advances in geology of the porphyry copper deposits, Southwestern North America: Tucson, University of Arizona Press, p.185-210.
- Einaudi, M.T. and Burt, D.M. 1982. Introduction, terminology, classification, and composition of skarn deposits: Economic Geology, v.77, p.745-754.
- Einaudi, M.T., Meinert, L.D. and Newberry, R.J.. 1981. Skarn deposits, *In:* Skinner, B.J., ed., Economic Geology 75th Anniversary Volume: El Paso Economic Geology Publishing Company, p.317-391.
- Elliott-Meadows, S.R. and Appleyard, E.C. 1991. The alteration geochemistry and petrology of the Lar Cu-Zn Deposit, Lynn Lake area, Manitoba, Canada: Economic Geology, v.86, p.486-505.
- Ettlinger, A.D., Meinert, L.D. and Ray, G.E. 1992. Gold skarn mineralization and fluid evolution in the Nickel Plate Deposit, British Columbia: Economic Geology, v.87, p.1541-1565.
- Eugster, H.P. 1986. Minerals in hot water: American Mineralogist, v.71, n.5/6, p.655-673.
- Farrar, E., Clark, A.H. Haynes, S.J., Quirt, G.S., Conn, H., Zentilli, M. 1970. K-Ar evidence for the migration of granitic intrusion foci in the Andes of Northern Chile: Earth and Planetary Science Letters, v.10, p.60-66.
- Kelly, J.M. 1975. Geology, wall-rock alteration and contact metamorphism associated with massive sulfide mineralization at the Amulet Mine, Noranda district, Quebec: Madison, Wisconsin, University of Wisconsin, unpubl. Ph.D thesis, 234p.
- Meinert, L.D. 1983. Variability of skarn deposits - Guides to exploration, *In:* Boardman, S.J., ed., Revolution in the earth sciences: Dubuque, Iowa, Kendall-Hunt Publishing Co., p.301-316.
- Meinert, L.D. 1984. Mineralogy and petrology of iron skarns in western British Columbia, Canada: Economic Geology, v.79, p.869-882.
- Meinert, L.D. 1988. Gold skarn deposits - a preliminary overview, *In:* Zachrisson, E., ed., Proceedings of the 7th quadrennial IAGOD symposium: Stuttgart, Schweizerbart'sche, p.363-374.
- Meinert, L.D. 1989. Gold skarn deposits - geology exploration criteria, *In:* Groves, D., Keays, R. and Ramsay, R. eds, The geology of gold deposits; the perspective in 1988: Economic Geology Monograph 6, p. 537-552.

- Mpodozis, C. and Ramos, V.A., 1990. The Andes of Chile and Argentina, In: Erickson, G.E. ed., Geology of the Andes and its relation to hydrocarbon and mineral resources: Earth Science Series, Circum-Pacific Council for Energy and Mineral Resources, v.11, p.59-90.
- Mpodozis, C. and Allmendinger, R., 1992. Extensión cretácea a gran escala en el Norte de Chile (Puquios-Sierra Fraga, 27°S); significado para la evolución tectónica de los Andes: Revista Geológica de Chile, v.19, n.2, p.167-197.
- Myers. G.L. 1990. Alteration zonation of the Fortitude gold skarn deposit, Lander County, NV: Mining Engineering, v.42, n.4, p.360-368.
- Ortíz. F.J., Araya, R., Franqueza, F., Moraga, B. and Zentilli, M., 1961. Informe geológico del Distrito Minera Punta del Cobre, Provincia de Atacama: Santiago, Instituto de Investigaciones Geológicas Chile, Publicación Especial, v.1.
- Pivot, P., and Johan, Z. 1982. Atlas of ore minerals: Paris, B.R.G.M. and Amsterdam, Elsevier, 458p.
- Riverin, G. and Hodgson, C.J. 1980. Wall-rock alteration at the Millenbach Cu-Zn Mine, Noranda, Quebec: Economic Geology, v.75, p.424-444.
- Sarkar, S.C., Bhattacharyya, P.K. and Mukherjee, A.D. 1980. Evolution of sulfide ores of Saladipura, Rajasthan, India: Economic Geology, v.75, p.1152-1167.
- Segerstrom, K. 1959. Geología del cuadrángulo Los Loros, Provincia de Atacama: Santiago, Instituto de Investigaciones Geológicas de Chile, Carta Geológica de Chile, v.1, n.1,, 33p.
- Segerstrom, K. 1960. Structural geology of an area east of Copiapó, Atacama Province, Chile: Copenhagen, 21st International Geological Congress, Part XVII, p.14-20.
- Segerstrom, K. and Parker, R.L. 1959. Geología del cuadrángulo Cerrillos, Provincia de Atacama: Santiago, Instituto de Investigaciones Geológicas de Chile, Carta Geológica de Chile, v.1, no.2, 33p.
- Segerstrom, K. and Ruiz, C. 1962. Geología del cuadrángulo Copiapó, Provincia de Atacama: Santiago, Instituto de Investigaciones Geológicas de Chile, Carta Geológica de Chile, v.3, no.1, 115p.
- Segerstrom, K., Thomas, H. and Tilling, R.I. 1963. Geología del cuadrángulo Pintadas, Provincia de Atacama: Santiago, Instituto de Investigaciones Geológicas de Chile, Carta Geológica de Chile, Carta no. 12, 52p.

Tilling, T.I. 1962. Batholith emplacement and contact metamorphism in the Paipote-Tierra Amarilla area, Atacama Province, Chile: Yale University, unpubl. Ph.D thesis, 202p.

Uytenboggardt, W. and Burke, E.A.J. 1971. Tables for microscopic identification of ore minerals: New York, Dover Publications, 430p.

Williams, S.A. 1990. Petrology of Candelaria Deposit: Phelps Dodge Mining Co. Chile, internal report, 2p.

Williams, S.A. 1994. Petrology of Candelaria Deposit: Phelps Dodge Mining Co. Chile, internal report, 2p.

Zentilli, M. 1974. Geological evolution and metallogenetic relationships in the Andes of northern Chile between 26° and 29° south: Kingston, Queen's University, unpubl. Ph.D thesis, 460p.

____oOo____